Monte-Carlo Methods in High-Altitude Aerodynamics

2

2.1 Basic Principle of Monte-Carlo Methods

The appearance of statistical simulation (Monte Carlo) methods in various fields of applied mathematics is usually caused by the appearance of qualitatively new practical problems. The examples include the creation of nuclear weapons, space development, the study of atmospheric optics phenomena, and the study of physicochemical and turbulence processes. One good definition is as follows: The Monte Carlo methods are the methods designed for solving mathematical problems (e.g., systems of algebraic, differential, or integral equations) based on the direct statistical simulation of physical, chemical, biological, economic, social, and other processes using the generation and transformation of random variables.

The first paper devoted to the Monte Carlo method was published as early as in 1873 [22]. It described the experimental determination of π by a realization of the stochastic process of tossing a needle on a sheet of ruled paper. A striking example is the use of von Neumann's idea to simulate the neutron trajectories in the Los Alamos laboratory in 1940. Although the Monte Carlo methods require a large amount of computations, the absence of computers at that time did not discourage the researchers. The name of these methods comes from the capital of the Principality of Monaco, which is famous for its Casino; indeed, the roulettes used in the casino are perfect tools for generating random numbers. The first paper [23] that systematically expanded this method was published in 1949. In that paper, the Monte Carlo method was used to solve linear integral equations. It could easily be guessed that these equations were related to the problem of the passage of neutrons through matter. In Russia, studies concerning the Monte Carlo methods appeared after the Geneva International Conference on the Peaceful Uses of Atomic Energy. One of the first Russian studies is [24].

The revelation of the methods of statistical modeling (Monte-Carlo) in various areas of the applied mathematics is connected as a rule with the necessity of solution of the qualitatively new problems, arising from the needs of practice. Such a situation appeared by the creation of the atomic weapon, at the initial stage of a mastering of space, by the investigation of the phenomena of atmospheric optics, the physical chemistry, and the modeling of turbulence flow (John von Neumann, Nicholas Constantine Metropolis, Stanislaw Marcin Ulam, Vasilii Sergeevich Vladimirov, Ilya Meerovitch Sobol, Gury Ivanovich Marchuk, Sergey Mikhailovich Ermakov, Gennady Alekseyevich Mikhailov, John Kenneth Haviland, Graeme A. Bird, Iain D. Boyd, Mikhail Naumovich Kogan, Vladimir Alexandrovich Perepukhov, Oleg Mikhaylovich Beloserkovskii, Yuri Ivanovich Khlopkov, Vitaliy Yevgenyevich Yanitskii, Mikhail Samuilovich Ivanov, Aleksandr Ivanovich Eropheev and et al.).

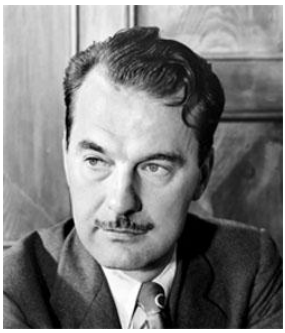

Metropolis N. C.

Ulam S. M.

Vladimirov V. S.

Beloserkovskii O. M.

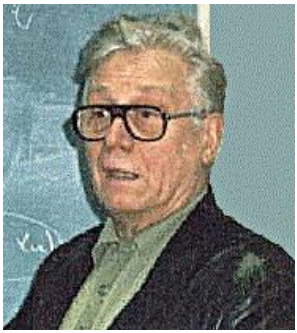

Ermakov S. M.

Mikhailov G. A.

Marchuk G. I.

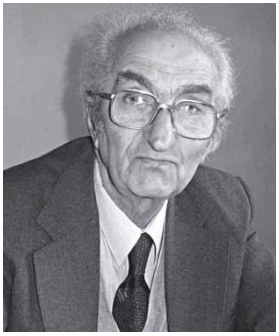

Kogan M. N.

Perepukhov V. A.

Bird G. A. and Khlopkov Yu. I.

The general scheme of the Monte Carlo method is based on the central limit theorem, which states that random variable

$$Y = \sum_{i=1}^{N} X_i$$

is equal to the sum of a large number of random variables with the same expectation m and the same variance σ^2 has the normal distribution with the expectation N and the variance $N\sigma^2$. Assume that we want to solve an equation or find the result of a certain process I. If we can construct the random variable ξ with the probability density $p(x)$ such that the expectation of this variable is equal to the unknown solution $M(\xi) = I$, then we obtain a simple method for estimating the solution and its error [25]:

$$I = \mathrm{M}(\xi) \approx \frac{1}{N}\sum_{i=1}^{N}\xi_i \pm \frac{3\sigma}{\sqrt{N}}$$

This implies the following general properties of the Monte Carlo methods:

1. The absolute convergence to the solution with the rate $1/N$.
2. An unfavorable dependence of the error ε on the number of trials: $\varepsilon \approx 1/\sqrt{N}$ (to reduce the error by an order of magnitude, the number of trials must by increased by two orders of magnitude).
3. The main method of reducing the error is the variance reduction; in other words, this is a good choice of the probability density $p(x)$ of the random variable ξ in accordance with the physical and mathematical formulation of the problem.
4. The error is independent of the dimensionality of the problem.

5. A simple structure of the computation algorithm (the computations needed to realize a proper random variable are repeated N times).

6. The structure of the random variable ξ can be generally based on a physical model of the process that does not require a formulation of the controlling equations as in regular methods; this fact is increasingly important for modern problems.

We illustrate the main features of the Monte Carlo methods and the conditions under which these methods outperform the conventional finite difference methods or are inferior to them using the following example. Suppose that we want to evaluate the definite integral of a continuous function over the interval [a, b]:

To evaluate this integral using the Monte Carlo method, we construct a random variable with the probability density $p(x)$ such that its expectation

$$\mathrm{M}(\xi) = \int_{-\infty}^{\infty} \xi p(x) dx$$

is equal to I. Now, if we set $\boldsymbol{\xi} = f(\mathbf{x})/p(\mathbf{x})$ within the integration limits, then we have, by the central limit theorem,

$$I = \frac{1}{N} \sum_{i=1}^{N} \xi_i \pm \frac{3\sigma}{\sqrt{N}}$$

On the one hand, the evaluation of I by formula described above can be interpreted as the solution of a mathematically stated problem; on the other hand, it can be interpreted as a direct simulation of the area under the plot of $f(\mathbf{x})$. The evaluation of the one-dimensional integral I_1 by the Monte Carlo method corresponds to the computation of I using the rectangular rule with the step $\Delta x \approx 1/\sqrt{N}$ and an error $O(\Delta \mathbf{x})$. If $f(x)$ is sufficiently "good", the integral I_1 in

the one-dimensional case can be calculated accurate to $O(\Delta x^2)$ using the trapezoid rule, accurate to $O(\Delta x^3)$ using the parabolic rule, and to any desired accuracy without a considerable increase in the computational effort. In the multidimensional case, the difficulties in using schemes of a high order of accuracy increase; for this reason, they are rarely used for the calculation of n-dimensional integrals I_n for $n \geq 3$.

Let us compare the efficiency of the regular and statistical methods for the problem described above. Let n be the dimensionality of the problem, Y be the number of nodes on an axis, $R = Y^n$ be the total number of nodes for the regular methods, q be the order of accuracy, N be the number of statistical trials, and ν be the number of operations needed to process one node (to perform one statistical trial). Then, $\varepsilon_L = Y^{-q}$ is the error of the regular methods, $\varepsilon_K = N^{-1/2}$ is the error of the statistical methods, $L(\varepsilon) = \nu R = \nu\varepsilon_L^{-n/q}$ is the number of operations when the problem is solved by a regular method, and $K(\varepsilon) = \nu N = \nu\varepsilon_K^{-2}$ is the number of operations when the problem is solved by the Monte Carlo method. Then, in the case of an equal number of operations needed to obtain a solution with the same accuracy using each of the methods, we have $n = 2q$. Therefore, for $n \geq 3$ and $q = 1$ (first-order schemes), the Monte Carlo methods are preferable. For other classes of problems, the relation between the efficiency of the methods can be different.

2.2 The Monte Carlo Methods in Computational Aerodynamics

The Boltzmann integro-differential kinetic equation for the single-particle distribution density is

$$\frac{\partial f}{\partial t} + \xi \nabla f = \int (f' f_1' - f f_1) \mathbf{g} b db d\varepsilon d\xi_1 = J(f) \tag{2.1}$$

here, $f = f(t, x, y, z, \xi_x, \xi_y, \xi_z)$ is the distribution density. f, f_1, f', f_1', correspond to the molecules with the velocities ξ, ξ_1 and ξ', ξ_1', before and after the collision, $\mathbf{g}$ is the relative velocity of the molecules in binary collisions $\mathbf{g} = |\mathbf{g}| = |\xi_1 - \xi|$, and b and ε are the impact parameter and the azimuth angle for the collision.

The complex nonlinear structure of the collision integral and the large number of variables (seven in the general case) present severe difficulties for the analysis including the numerical analysis. The high dimension, the probabilistic nature of the kinetic processes, and complex molecular interaction models are the natural prerequisites for the application of the Monte Carlo methods. Historically, the numerical statistical methods in rarefied gas dynamics developed in three directions:

1. The use of the Monte Carlo methods to evaluate the collision integrals in the regular finite difference schemes for solving the kinetic equations.

2. The direct statistical simulation of physical phenomena, which is subdivided into two approaches: the simulation of trajectories of test particles by the Haviland method [26] and the simulation of the evolution of the ensemble of particles by the Bird method [27].

3. The construction of a stochastic process using the Ulam–Neumann procedure [28] corresponding to the solution of the kinetic equation.

The hierarchy of levels of the description of large molecular systems includes a wide range of approaches, and various descriptions of the molecular dynamics at

different levels can be used for constructing efficient statistical simulation methods.

The most detailed level of description is a dynamical system. To describe a system consisting of a large number N of particles (a molecular gas is a system of this kind), one must specify the initial coordinates and velocity of each molecule r_j, x_j and the evolution equations of this system

$$m\frac{d^2\mathbf{r}_j}{dt^2}=\sum_{i\neq j}^{N}R_{ij} \tag{2.2}$$

The solution of such a system is an unrealizable (cannot be solved in practice) problem even for a very rarefied gas. Indeed, at a height of 400 km (the most popular satellite orbits), one cubic centimeter contains 10^9 molecules. For this reason, a less detailed statistical description is used.

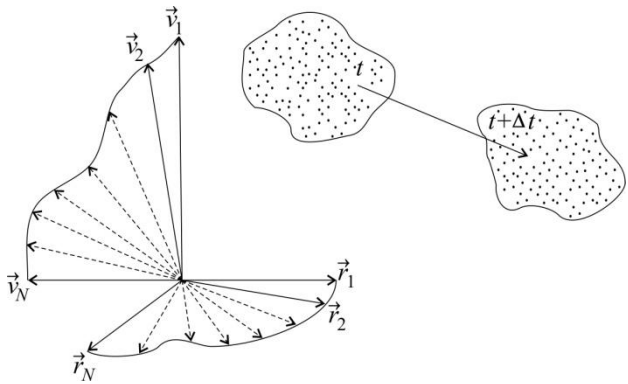

Figure 2.1 *Dynamical system of molecules.*

Following the Gibbs formalism, rather than consider a single system, an ensemble of systems in the 6N-dimensional Γ-space distributed according to the N-particle distribution function $f(t,\mathbf{r}_1,...,\mathbf{r}_N,\xi_1,...,\xi_N)=f_N$ is considered. This

function is interpreted as the probability of finding the system in the neighborhood $dr_1 \ldots dr_N d\xi_1 \ldots d\xi_N$ of the point $r_1, \ldots, r_N, \xi_1, \ldots, \xi_N$ at the moment t:

$$dW = f_N d\mathbf{r}_1 .. d\mathbf{r}_N d\boldsymbol{\xi}_1 ... d\boldsymbol{\xi}_N$$

Such an ensemble is described by the Liouville equation

$$\frac{\partial f_N}{\partial t} + \sum_{i=1}^{N} \boldsymbol{\xi}_i \frac{\partial f_N}{\partial \mathbf{r}_i} + \sum_{i \neq j}^{N} \sum_{i=1}^{N} \frac{F_{ij}}{m} \frac{\partial f_N}{\partial \boldsymbol{\xi}_i} = 0 \qquad (2.3)$$

From now on, the Liouville equation and all the subsequent kinetic equations following from the Bogolyubov chain including the last Boltzmann equation have a probabilistic nature. Although Eq. (2.3) is simpler than system (2.2), it takes into account the collisions of N molecules and is very difficult to analyze. A less detailed description is achieved by roughening the description using s-particle distribution function $f_s = \int f_N d\mathbf{r}_{s+1} ... d\mathbf{r}_N d\boldsymbol{\xi}_{s+1} ... d\boldsymbol{\xi}_N$, which determine the probability to simultaneously find s particles independently of the state of the remaining (N–s) particles.

Following Bogolyubov's ideas, we obtain the chain of linked equations

$$\frac{\partial f_s}{\partial t} + \sum_{i=1}^{s} \boldsymbol{\xi}_i \frac{\partial f_s}{\partial \mathbf{r}_i} + \sum_{i=1}^{s} \sum_{j=1}^{s} \frac{F_{ij}}{m} \frac{\partial f_s}{\partial \boldsymbol{\xi}_i} = -\sum_{i=1}^{s} (N - s) \frac{\partial}{\partial \boldsymbol{\xi}_i} \int \frac{F_{ij}}{m} f_{s+1} d\mathbf{r}_{s+1} d\boldsymbol{\xi}_{s+1} \qquad (2.4)$$

up to the single-particle distribution function $F_1 = f(t, r, \xi)$ corresponding to the Boltzmann gas, which only takes into account the binary collisions:

$$\frac{\partial f_2}{\partial t} + \sum_{i=1}^{2} \boldsymbol{\xi}_i \frac{\partial f_2}{\partial \mathbf{r}_i} + \sum_{i=1}^{2} \sum_{j=1}^{2} \frac{F_{ij}}{m} \frac{\partial f_2}{\partial \boldsymbol{\xi}_i} = -\sum_{i=1}^{2} (N - 2) \frac{\partial}{\partial \boldsymbol{\xi}_i} \int \frac{F_{ij}}{m} f_{2+1} d\mathbf{r}_{2+1} d\boldsymbol{\xi}_{2+1}$$

For triple collisions:

$$\frac{\partial f_3}{\partial t}+\sum_{i=1}^{3}\xi_i\frac{\partial f_3}{\partial \mathbf{r}_i}+\sum_{i=1}^{3}\sum_{j=1}^{3}\frac{F_{ij}}{m}\frac{\partial f_3}{\partial \xi_i}=-\sum_{i=1}^{3}(N-3)\frac{\partial}{\partial \xi_i}\int\frac{F_{ij}}{m}f_{3+1}d\mathbf{r}_{2+1}d\xi_{3+1}$$

Following Boltzmann, we assume that the molecules are spherically symmetric and accept the molecular chaos hypothesis $F_2(t, r_1, r_2, \xi_1, \xi_2) = F_1(t, r_1, \xi_1)\, F_1(t, r_2, \xi_2)$ to obtain Eq. (2.1).

It is very interesting to consider a particular case of Liouville's equation (2.3) and of Bogolyubov's chain (2.4) that describe a spatially homogeneous gas consisting of a bounded number of particles and corresponding to two-particle collisions; in this case, on the final link of the chain, we obtain the Kac master equation [29]

$$\frac{\partial \varphi_1(t,\xi_1)}{\partial t}=\frac{N-1}{N}\int\left[\varphi_2(t,\xi_1',\xi_2')-\varphi_2(t,\xi_1,\xi_2)\right]\mathbf{g}_{12}d\sigma_{12}d\xi_2 \qquad (2.5)$$

where φ_1 and φ_2 are the one- and two-particle distribution functions. In contrast to the Boltzmann equation, Eq. (2.5) is linear, which will be used in the development and justification of efficient numerical direct statistical simulation schemes.

Returning to the Boltzmann equation, we easily obtain all the macroscopic parameters from the definition of the function *f*. For example, the number of molecules *n* in a unit volume of the gas is

$$n(t,\mathbf{r})=\int f(t,\mathbf{r},\xi)d\xi$$

The mean velocity of the molecules, the strain tensor, and the energy flux are determined by the relations

$$\mathbf{v}(t,\mathbf{r})=\frac{1}{n}\int\xi f(t,\mathbf{r},\xi)d\xi\,,$$

$$P_{ij} = m\int c_i c_j f(t,\mathbf{r},\boldsymbol{\xi})d\boldsymbol{\xi},$$

$$q_i = \frac{m}{2}\int c^2 c_i f(t,\mathbf{r},\boldsymbol{\xi})d\boldsymbol{\xi},$$

where $c = \boldsymbol{\xi} - V$ is the thermal velocity of the molecules. The mean energy of the heat motion of molecules is usually described in terms of the temperature

$$\frac{3}{2}kT = \frac{1}{n}\int \frac{mc^2}{2} f(t,\mathbf{r},\boldsymbol{\xi})d\boldsymbol{\xi}$$

Applying the Chapman–Enskog procedure to the Boltzmann equation, we obtain the hydrodynamical level of description. This sequentially yields the Euler, Navier–Stokes, Barnett, etc., equations:

$$\frac{\partial \rho}{\partial t} + \frac{\partial \rho V_i}{\partial x_i} = 0$$

$$\left(\frac{\partial}{\partial t} + V_j \frac{\partial}{\partial x_j}\right) V_i = -\frac{1}{\rho}\frac{\partial P_{ij}}{\partial x_j}$$

$$\frac{3}{2}R\rho\left(\frac{\partial}{\partial t} + V_j \frac{\partial}{\partial x_j}\right) T = -\frac{\partial p_j}{\partial x_j} - P_{ij}\frac{\partial V_j}{\partial x_j}$$

$$p_{ij} = \mu\left(\frac{\partial V_i}{\partial x_j} + \frac{\partial V_j}{\partial x_i} - \frac{2}{3}\delta_{ij}\frac{\partial V_r}{\partial x_r}\right)$$

$$q_i = -\lambda\frac{\partial T}{\partial x_i}.$$

$$p = \rho RT$$

The expressions for the components of the thermal velocity can be obtained by simulating the normally distributed random variable

$$\xi_x = \sqrt{\frac{2k_B T}{m}} \sqrt{-\ln \alpha_1} \cos(2\pi\alpha_2)$$

$$\xi_y = \sqrt{\frac{2k_B T}{m}} \sqrt{-\ln \alpha_1} \sin(2\pi\alpha_2)$$

$$\xi_z = \sqrt{\frac{2k_B T}{m}} \sqrt{-\ln \alpha_3} \cos(2\pi\alpha_4)$$

here, α_k is independent random numbers that are uniformly distributed on the interval (0, 1). In order to reproduce the mean velocity more accurately, it is reasonable to use the following symmetrized algorithm: the thermal velocities of the particles with the odd indexes are calculated, and the thermal velocities of the particles with the even indexes are set equal to the velocities of the corresponding odd particles with the opposite sign.

The complex nonlinear structure of the collision integral and the large number of variables (seven in the general case) present severe difficulties for the analysis including numerical analysis. The high dimension, the probabilistic nature of the kinetic processes, and complex molecular interaction models are the natural prerequisites for the application of the Monte Carlo methods [25, 30].

Let's see the kinetic equations for triple molecular collisions. The statistical independence of particles before collision, solution of equation is [31]

$$f_3(t, \tau_1, \tau_2, \tau_3) = f_1(t_0, \tau_{10}) f_1(t_0, \tau_{20}) f_1(t_0, \tau_{30}) .$$

where $\tau_{a0} = \tau_{a0}(t, t_0, \tau_1, \tau_2, \tau_3)$ – coordinate and impulse values which particles at the moment t_0 for that at the time t get into given points τ_1, τ_2, τ_3 of the phase space.

Now, let's move from f_1 to $f = Nf_1$, and find kinetic equation in the form of

$$\frac{\partial f}{\partial t} + \bar{\xi}\nabla f = St_2 f + St_3 f \ ,$$

- $St_2 f(t,\tau_1) = \int \frac{\partial F_{12}}{m} \frac{\partial}{\partial \xi} \{S_{12} f(t,\tau_1) f(t,\tau_2)\} d\tau_2$ - Integral for pair collisions,

- $St_3 f(t,\tau_1) = \frac{1}{N} \int \frac{F_{12}}{m} \frac{\partial}{\partial \xi} \{R_{123} f(t,\tau_1) f(t,\tau_2) f(t,\tau_3)\} d\tau_2 d\tau_3$ - Integral for triple collision,

here S_{12} and R_{123} – some operators. Let's consider a few of collision processes taking into account integral. First of all, the operator R_{123} is zero, if at least one of the particles does not interact with the others. The process $R_{123} \neq 0$ is not only the triple collisions, but also combination of several pair of molecules. We consider several types of collisions (Figure 2.2 (a, b, c)) [31].

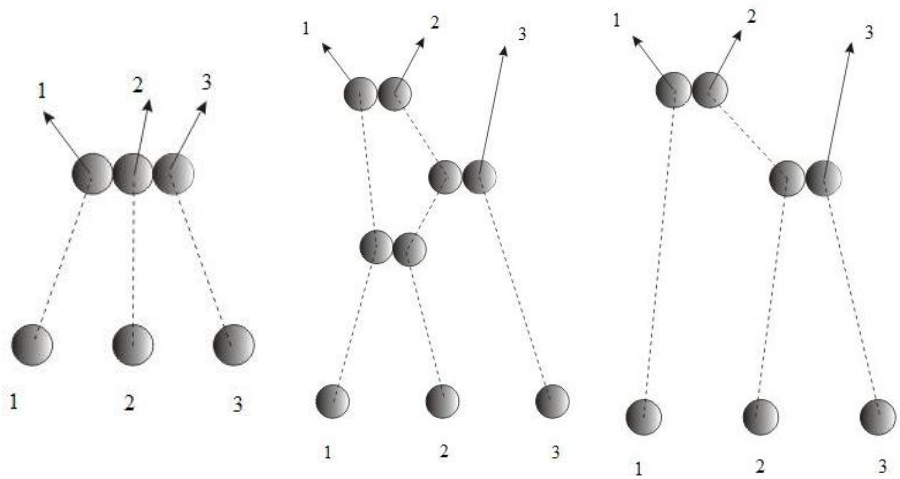

(a) *(b)* *(c)*

Figure 2.2 *The basic trajectories of triple collisions of molecules.*

Figure 2.3 show the distribution of the velocity of the molecules before and after collisions (total number of particles $N = 9\times10^5$). From the graphs, it is clear that the velocity distribution of the molecules before and after collision is the same. Elastic collision is defined as collision in which there is no exchange between the translational and internal energies. Triple collisions will occur, after colliding as pair molecular collisions. Although the Lennard-Jones potential and is used in simulations of liquid and solids, strictly speaking, the molecular interaction at high densities is no longer a pair collision [32].

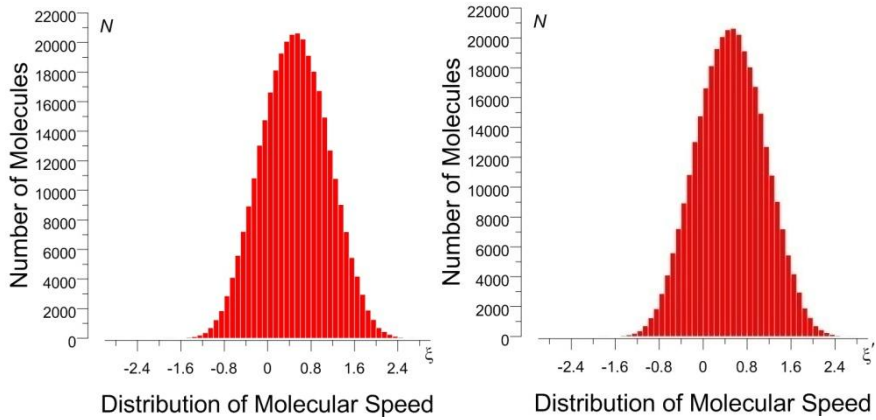

Figure 2.3 *Velocity distribution function before and after collisions.*

In condensed mediums, to consider the collisions of molecules, the environment effects on the molecules. So, the solid argon contribution to the energy of the triple collisions can reach 10% [33]. However, taking into account the triple collisions of molecules computationally too expensive to simulate in rarefied gas dynamics approach [34-36].

2.3 Method for Surface Description of the Complex Vehicle Design

One of the basic technology questions of aerodynamic characteristics calculation of the arbitrary apparatus shape is the rational choice of way to describe of surface geometry. Methods for describing of complex surfaces can be divided into two main groups: mathematical approximation of a surface and space distribution of large number surface points which restored the system of surface element. The main disadvantage of the first group of methods are usually related to approximation of complex mathematical problems, essentially nonlinear surfaces on small number of control points, and the second - difficulty preparation of initial data. In the given work, these both methods are used: due to comparative simplicity and universality of the task of control points, and finally restore surface on the control points, the modeled body is divided into number of specific parts (wing, fore part, bottom-most part of fuselage, etc.), for each of those is conducted square-law interpolation on control points [37].

For each part introduces the axis (x, y', z'), which are the axes of the symmetric coordinate system. Axis divided into a finite number of characteristic points defined by the parameters x_i, y_i, z_i. These points in a cylindrical coordinate system are given by section: φ_j, R_{ij}; φ_{yi}, R_{yij}; φ_{zi}, R_{zij}. Depending on the shape of the cross section, it can be defined as a discrete and in analytical form.

For qualification the surface of the passing points provides an interpolation procedure. Intermediate points on the axes and the angles are according to the formulas of the linear interpolation,

$$x_i = \frac{1}{2}\left(x_{\frac{i-1}{2}} + x_{\frac{i+1}{2}} \right),$$

$$\varphi_j = \frac{1}{2}\left(\varphi_{\frac{j-1}{2}} + \varphi_{\frac{j+1}{2}}\right)$$

Radius value by use of Lagrange polynomial interpolation is interpolated twice – by φ и x:

$$R(a) = \sum_{i=1}^{3} R(a_i) \prod_{j \neq 1} \frac{a - a_j}{a_i - a_j}$$

where $a_{i,,j}$ - correspond to the values of φ и x in the interpolation points.

Thus, with the required accuracy are given by the initial points on the surface. The question remains, how is spanned by the available core surface of the streamlined apparatus. As already noted, the aim is suitable linear approximation, so in the capacity of basic will consider the linear element, correspond triangle, which was built by nearest three points. Vertices of triangles in rectangular coordinates for the different parts are defined by formula.

For fuselage

$$r = \begin{pmatrix} x \\ y \\ z \end{pmatrix} = \begin{pmatrix} x_i \\ R_{ij} \cos\varphi_j \\ R_{ij} \sin\varphi_j \end{pmatrix}$$

For wing

$$\begin{pmatrix} x \\ y \\ z \end{pmatrix} = \begin{pmatrix} x_0 + z_i \cos\alpha_z - R_{zij} \cos\gamma_{zi} \\ y_0 + z_i \sin\alpha_z + R_{zij} \sin\varphi_{zj} \\ z_0 + z_i \cos\alpha_z \cos\beta_z - R_{zij} \cos\varphi_{zj} \sin\gamma_{zi} \end{pmatrix}$$

Where (x_0, y_0, z_0) - initial coordinates of the axis of the wing z', α_z – angle of slope of axis of the wing to the surface $y = 0$, β_{zi} - angle of slope of the axis of the

wing to the axis z, γ_{zi} - the angle of slope defined by sections on the axis z'. For full definition of elements it is necessary to determine its orientation and surface area.

Let a = $r_2 - r_1$, b = $r_3 - r_1$, generating elements of the vector. Then element of the area and normal to the surface

$$S=\frac{1}{2}(a\times b),$$

$$n=(a\times b)/(|a\times b|)$$

An estimate error for approximation by linear elements in the process for free molecular flow regime gives good results. So, for the approximation in calculation the resistance of cone accurate within 5% (average error of statistical methods) should be about 10 elements, and for approximation of the sphere – 100, single application of the interpolation procedure reduces the error by an order [37].

2.4 The Mathematical Description of Gas-Surface Interaction Models

The collision process between gas molecule and solid surface is termed gas-surface interaction. In kinetic theory, the gas-surface interaction forms a boundary condition between the gas molecules and solid surface. For scales relevant to kinetic theory, the gas-surface interactions are usually modeled with parameters having macroscopic character, in order to have manageable and efficient calculations. Although various gas-surface interaction models have been proposed over the past century and a half, the validity of these models remains tenuous for rarefied gas flow condition. In particularly, intended to analyze gas-surface interaction models on aerodynamic effects (Maxwell model, Cercignani-Lampis-Lord (CLL) model and Lennard-Jones potential).

The majority of gas dynamic problems include the interaction of gas particles with the body surface. Diffusion reflection with complete momentum and energy accommodation is most frequently used in DSMC method. In a diffuse reflection, the molecules are reflected equally in all directions usually with a complete thermal accommodation. The problem of gas-surface interaction takes an essential place in aerodynamics. The role of laws of molecular interaction with surfaces is shown more strongly, than more gas is rarefied [32]. Boundary conditions for Boltzmann equation are the conditions relating the distribution function of incident and reflected molecules.

2.4.1 Maxwell Model

The most popular gas-surface interaction model for kinetic theory is specular and diffuse reflection model developed by Maxwell (1879). This model is based on the assumption that the portion $(1-\sigma_\tau)$ of molecules reflected specularly from the surface, and the rest part σ_τ of the molecule diffusely. The density of distribution of reflected molecules is set as follows:

$$f_r(\mathbf{x}_w,\xi_r)=(1-\sigma_\tau)\,f_i\left(\mathbf{x}_w,\xi_r-2(\xi_r\cdot\mathbf{n})\mathbf{n}\right)+\sigma_\tau\,n_r\pi^{-3/2}h_r^{3/2}\exp\left(-h_r\xi_r^2\right),\ (\xi_r\cdot\mathbf{n})>0$$

and the scattering kernel has form

$$K(\xi_i\to\xi_r)=(1-\sigma_\tau)\delta\left[\xi_i-2\left(\xi_r\cdot\mathbf{n}\right)\mathbf{n}\right]-\sigma_\tau\frac{2h_r^2}{\pi}\exp\left[-h_r\xi_r^2\right]\cdot\left(\xi_i\cdot\mathbf{n}\right),\quad h_r=\frac{m}{2kT_r}$$

Here, ξ_r –velocity vector of the reflected molecules, δ – Dirac delta-function, n –outward unit normal to the surface x_w, h_r - most probable velocity of molecules at temperature T_w. Indexes *i* and *r* denote the quantities for the incident and reflected fluxes, and an index *w* - the value corresponding to diffuse reflection at

temperature of wall T_w. Parameter $0 \le \sigma_\tau \le 1$ in Maxwell model defines accommodation coefficient for the tangential momentum.

$$\sigma_\tau = \frac{p_{i\tau} - p_{r\tau}}{p_{i\tau}}$$

For complete specular reflection $\sigma_\tau = 0$, for complete diffuse reflections $\sigma_\tau = 1$. Popularity of Maxwell model is due to its simplicity and with the fact that it satisfies the principle of detailed balance. Maxwell's model proved suitable for low speed experiments and low rarefaction environments.

The velocity vector components at diffuse reflection are modelled in local spherical coordinate system which axis is directed along outward unit normal to the surface, by means of expressions [30]

$$|\xi_r| = h_r^{-1/2}\sqrt{-\ln(\alpha_1\alpha_2)}, \quad \cos\theta = \sqrt{\alpha_3}, \quad \varphi = 2\pi\alpha_4$$

Where α_1, α_2, α_3, α_4 - the independent random numbers uniformly distributed between 0 and 1. θ, φ - polar and azimuthal angles. The Accommodation coefficient of kinetic energy is defined in terms of incident and reflected fluxes as follows

$$\sigma_E = \frac{E_i - E_r}{E_i - E_w} = \frac{\xi_i^2 - \xi_r^2}{\xi_i^2 - h_w^{-1}}$$

Here E_w - energy which would be carried out the reflected molecules if gas is in equilibrium with wall, i.e., when $T_r = T_w$. Expression for velocity of the reflected molecule corresponding to not full accommodation of kinetic energy looks like

$$|\xi_r| = kh_r^{-1/2}\sqrt{-\ln(\alpha_1\alpha_2)}, \quad k = \sqrt{(1-\sigma_E)\xi_i^2 h_r + \sigma_E}$$

2.4.2 Cercignani-Lampis-Lord Model

In work [38] is proposed phenomenological model of Cercignani-Lampis (CL) which also satisfies to principle of reciprocity and is reported improvement of the Maxwell models [32]. The model is based on introduction of two parameters which represent accommodation coefficient of kinetic energy connected with coefficients of normal momentum $\sigma_n = \sigma_{En}$, and tangential momentum accommodation σ_τ, respectively.

Model CL well corresponds to results of laboratory researches with high-speed molecular beams. Although comparison is limited by laboratory conditions, CL model is theoretically justify and relatively simple. Later, there were modification of scattering kernel of CL model; however, they give slight improvement at comparison with laboratory experiments. Generally the interaction model has some arbitrary physical parameters that allow to achieve the reasonable agreement with results of laboratory researches in range of conditions. In this sense, original model CL is enough physical and suitable for theoretical research. The universal model should use the scattering kernel received on the basis of physical experiment in a wide range of Knudsen numbers and velocity of stream.

In CL model, the diffusion kernel of velocity for surface normal has the following form

$$K(\xi_{ni} \to \xi_{nr}) = \frac{2\xi_{nr}}{\sigma_n} I_0\left(2\sqrt{1-\sigma_n}\frac{|\xi_{ni}|\xi_{nr}}{\sigma_n}\right)\exp\left[-\frac{\xi_{nr}^2 + (1-\sigma_n)\xi_{ni}^2}{\sigma_n}\right]$$

$$I_0(x) = \frac{1}{2\pi}\int_0^{2\pi} \exp(x\cos\phi)d\phi$$

Here I_0 –first type Bessel function, ξ_{ni}, ξ_{nr} – molecular velocities of surface normal for the incident and reflected molecules, rating as $h_w^{-1/2}$. A scattering kernel is written as follow

$$K(\xi_{\tau i} \to \xi_{\tau r}) = \frac{1}{\sqrt{\pi\sigma_\tau(2-\sigma_\tau)}} \exp\left[-\frac{\left(\xi_{\tau r} - (1-\sigma_\tau)\xi_{\tau i}\right)^2}{\sigma_\tau(2-\sigma_\tau)}\right]$$

Here $\xi_{\tau i}$, $\xi_{\tau r}$ – molecular velocities of tangent to surface for the incident and reflected molecules, rating as $h_w^{-1/2}$.

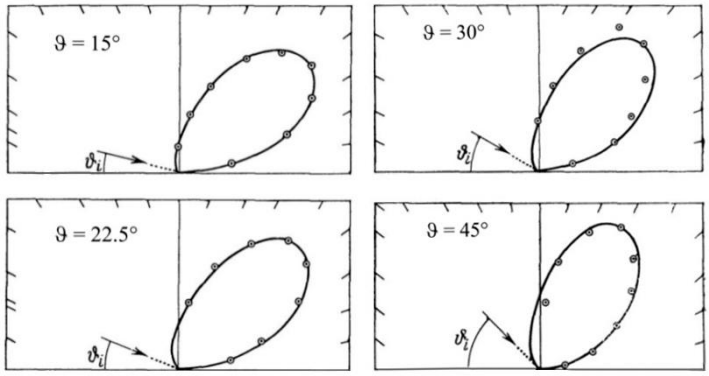

Figure 2.4 *Comparison of the experimental data of [39] with the calculated results by using the kernel [38].*

(σ_n = 0.3, σ_τ = 0.1, θ = 15°, 22.5°, 30° and 45°)

Twenty years after creation CL model have been published the algorithm of its realization based on some transformation with the limits of direct statistic simulation method [40]. The model in this form is called as Cercignani-Lampis-Lord model (CLL). Usage of CL model transformation expands to account for rotational energy exchange between gas and surface. Then, updating CLL model in the form of [41] is to account for vibrational energy

exchange and extend rang of states of the scatted molecule. CLL model is widely recognized examples of its application are presented in multiple works [42-55].

In order to simulate the partial surface accommodation, the CLL model was implemented into this DSMC calculation [56]. The CLL model is derived assuming momentum components. The two adjustable parameters appearing in the CLL model are the normal component of translational energy α_n and the tangential component of momentum σ_τ. However, in the implementation of the CLL model in the DSMC method, Bird has shown that it is equivalent to specify the normal α_n and tangential α_τ components of translational energy, since $\alpha_\tau=\sigma_\tau(2-\sigma_\tau)$, and thus $\sigma_\tau<\alpha_\tau$, assuming that σ_τ lies between 0 and 1.

2.4.3 Nocilla Model

The model (Nocilla, 1963) [57] was for the first time applied to the calculation of aerodynamic coefficients of drag and lift for simple figures in a free-molecular flow. The model is more general as compared to the Maxwell model; but at the same time, it is also simple in application. We can see more about explanation about Nocilla model in the work [58-63].

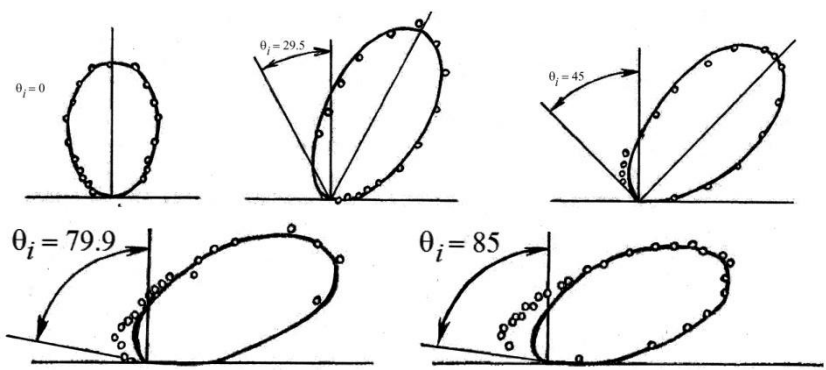

Figure 2.5 *Comparison of the experimental data [32].*

The distribution functions of the particles reflected from the surface are presented in the following form:

$$f_r = n_r\left(\frac{\pi}{h_r}\right)^{3/2}\exp\left\{-\left[(h_r)^{1/2}\xi_y - S_{nr}\right]^2 - \left[(h_r)^{1/2}\xi_x - S_{\tau r,x}\right]^2 - \left[(h_r)^{1/2}\xi_z - S_{\tau r,z}\right]^2\right\}$$

here ξ, n_r are the velocity and density of reflected molecules, and S_{nr}, $S_{\tau r}$ are the velocity vector components of incident molecules. Parameters of the function f_r are selected depending on available experimental data and the law of mass conservation.

$$S_{nr} = 0.1 - 0.65\frac{2\theta}{\pi},$$

$$S_{\tau r,x} = \frac{\tau_{r,x}}{p_r}\cdot\frac{J_2(S_{nr})}{J_1(S_{nr})},\quad 2\frac{k}{m}T_r = \left(\frac{p_r}{q_{mr}}\right)2\left[\frac{J_1(S_{nr})}{J_2(S_{nr})}\right]^2,$$

$$n_r = q_{mr}\left(2\frac{k}{m}T_r\right)^{-1/2} J_1^{-1}(S_{nr}),$$

$$\tau_{r,x} = -\left(a_\tau + b_\tau\frac{4\theta-\pi}{2\pi}\right)q_{mi}\ \xi\ \sin\theta,$$

$$p_r = \left\{\left(a_n + b_n\frac{2\theta}{\pi}\right)\xi + \left(\frac{\pi}{2}\frac{kT_w}{m}\right)^{1/2}\right\}q_{mi},$$

$$J_1(t) = \frac{1}{\sqrt{\pi}}\int_0^\infty q\exp\left[-(q-t)2\right]dq = \frac{1}{\sqrt{2\pi}}\left[e^{-t^2} + \sqrt{\pi}\,t(1+erf\,(t))\right],$$

$$J_2(t) = \frac{1}{\sqrt{\pi}}\int_0^\infty q^2\exp\left[-(q-t)2\right]dq = \frac{1}{\sqrt{2\pi}}\left[te^{-t^2} + \sqrt{\pi}\left(\frac{1}{2}+t^2\right)(1+erf\,(t))\right],$$

$$erf\,(t) = \frac{2}{\sqrt{\pi}}\int_0^t e^{-s^2}ds,\quad q_{mr} = q_{mi} = mq_1;\quad q_1 = 1\left[m^{-2}s^{-1}\right].$$

here, θ – angle between velocity vector of incident and internal normal to the surface, T_r – wall temperature, q_{mr}, q_{mi} – incident and reflected flux, which are used by normal distribution function f_r in Monte-Carlo method. The parameters a_n, b_n, a_τ and b_τ depends on material of surface which obtained from experimental work. The Nocilla model is use in the complex program "SMILE" [64] and "MONACO" for spacecraft aerodynamics investigation [65].

2.4.4 Lennard-Jones Potential

Generally speaking, at molecular level it is necessary to consider interaction potentials, using electron-nuclear representations. Empirical potential dependences reflect the fact, that attractive forces at large distance and repulsive forces at short distances. This feature is reflected most simply with Lennard-Jones potential. The sixth power is decrease of potential simulate electro-statistical dipole-dipole and dispersive attraction. The twelfth-power repulsive potential is decrease from reasons of mathematical convenience. At the same time, it models rigid enough repulsion.

$$U(r) = 4\varepsilon\left[\left(\frac{\sigma}{r}\right)^{12} - \left(\frac{\sigma}{r}\right)^{6}\right]$$

when $r = \sigma$ the potential is equal to zero.

The value ε characterizes depth of a potential hole of the one electron volt. This feature is most simply reflects Lennard-Jones potential. It's shown that this model qualitatively correctly described the behavior of aerodynamic characteristics [32].

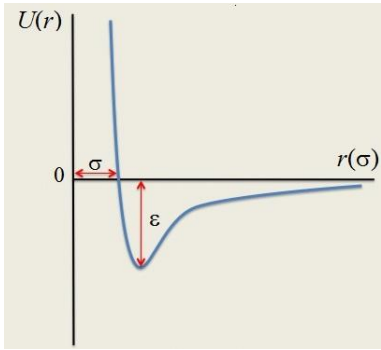

Figure 2.6 *Lennard-Jones potential.*

2.5 Modelling of the Aerodynamic Characteristics of Aerospace Vehicles in Free Molecular Flow

The calculation has been carried out through the method described in the previous section within the range of angles of attack α from – 90 deg to + 90 deg with a step of 5 deg. The parameters of the problem are the following: ratio of heat capacities γ = 1.4; temperature factor $t_w = T_w/T_0$ = 0.04; velocity ratio M_∞ = 20, energy accommodation coefficient σ_n = 0.5, 0.9, 1, momentum accommodation coefficient σ_τ = 0.5, 0.9, 1. The coefficients of drag force C_x, lift force C_y and pitching moment m_z which are calculated according to equations as below

$$C_i = \frac{F_i}{\frac{1}{2}\rho_\infty V_\infty{}^2 S_{ref}}, \quad m_Z = \frac{M_i}{\frac{1}{2}\rho_\infty V_\infty{}^2 L_{ref} S_{ref}}, \qquad i = x, y, z$$

L_{ref}, S_{ref} – references length and surface; F_i, M_i – *resultant force acting on the vehicle and moment, respectively.*

In the figure 2.8 presented the results of the calculation of the coefficients of drag force C_x, lift force C_y with value of angle of attack α from 0 deg to 30 deg for

reentry vehicle (Figure 2.7) by using DSMC method with the use of three gas-surface interaction models (Maxwell, Cercignani-Lampic-Lord).

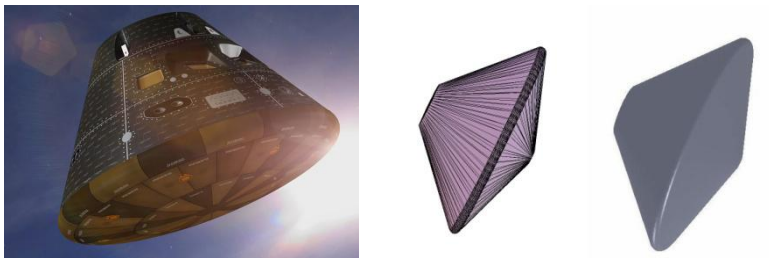

Figure 2.7 *General view and schematic view of reentry vehicle.*

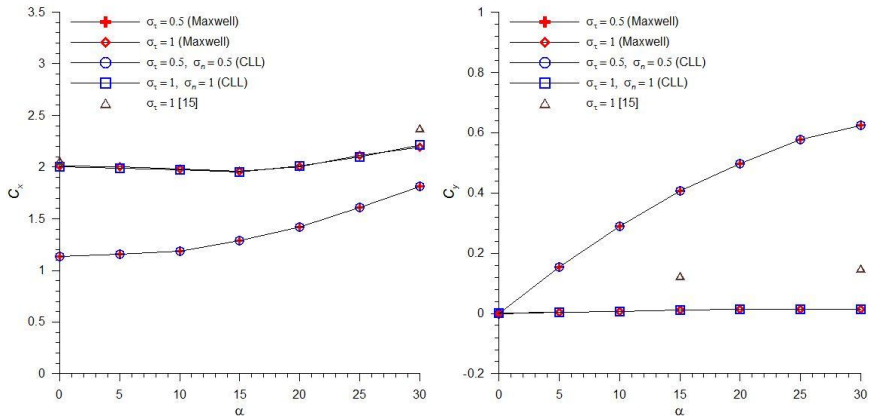

Figure 2.8 *Dependencies of C_x (α) and C_y (α) for reentry vehicle.*

In the Figure 2.10 presented the results of the calculation of the coefficients of drag force C_x, lift force C_y with value of angle of attack α from – 90 deg to + 90 deg for aerospace vehicles (Figure 2.9) by using DSMC method with the use of three gas-surface interaction models. In several works (Vaganov A. V., Drozdov S., Kosykh A. P., Nersesov G. G., Chelysheva I. F., Yumashev V. L., Khlopkov Yu. I., Voronich I. V., Zay Yar Myo Myint, Khlopkov A. Yu.) investigated the aerodynamics characteristics of aerospace vehicle "Clipper, model of TsAGI" [66, 48-45].

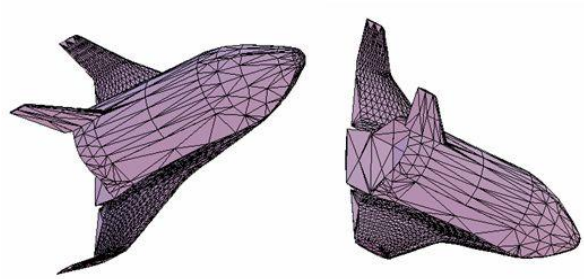

Figure 2.9 *Geometrical view of aerospace vehicle "Clipper".*

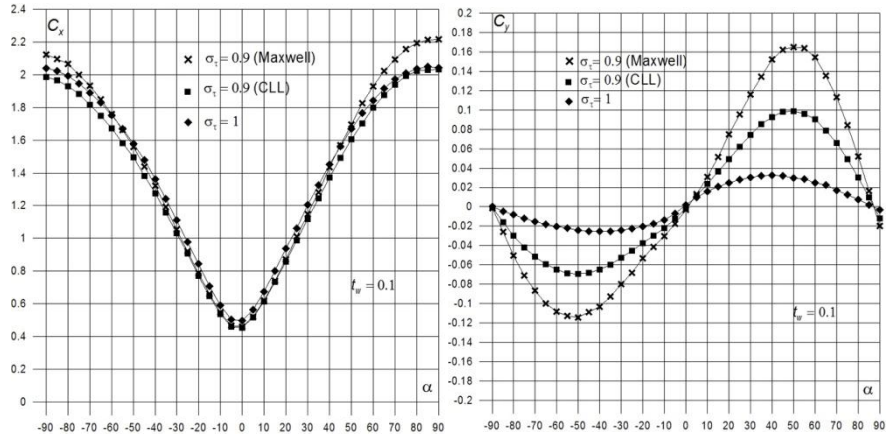

Figure 2.10 *Dependencies of C_x (α) and C_y (α) for aerospace vehicle "Clipper".*

From these results, we can explain, the drag and lift coefficient results of CLL model less than the Maxwell model as expected. The Maxwell model and CLL model predict the same lift, drag when the accommodation coefficients are equal to zero or one. In fact, for $\alpha_\tau = 1$ in Maxwell model and $\alpha_\tau = \alpha_n = 1$ in the CLL model, the two models give precisely the same. For accommodation coefficients not equal to zero or one, the CLL model gives higher aerodynamic forces than the Maxwell model for the same value of their respective accommodation coefficients.

In figure 2.11 shows the dependence of $C_x(\alpha)$ and heat transfer coefficient C_h with the use of various gas-surface interaction models (Maxwell,

Cercignani-Lampic-Lord (CLL), Lennard-Jones (LJ)). In this reason, the accommodation coefficient σ_τ is 1. Coefficient C_x increases with the rise of the angle of attack. From the graphs, it is clear that the coefficients are sensitively different at models of the gas-surface interaction models with surfaces.

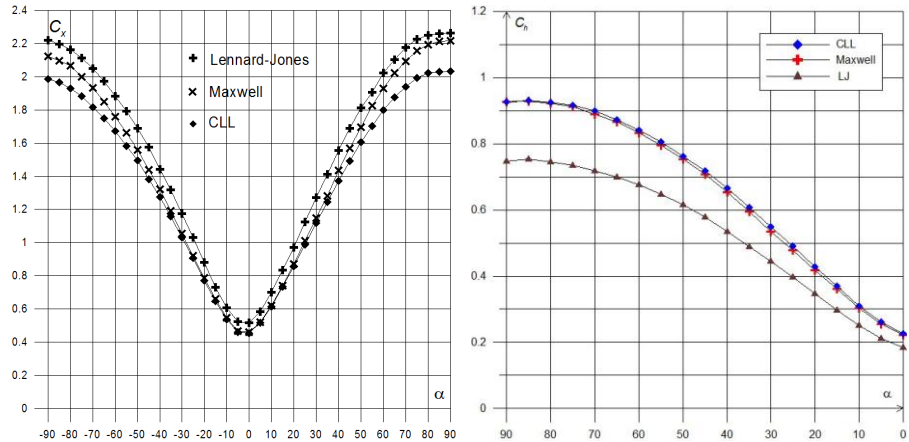

Figure 2.11 *Dependencies of $C_x(\alpha)$ and $C_h(\alpha)$ for aerospace vehicle with various gas-surface interaction models.*

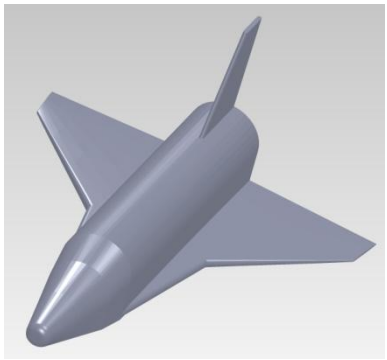

Figure 2.12 *Geometry view of aerospace vehicle.*

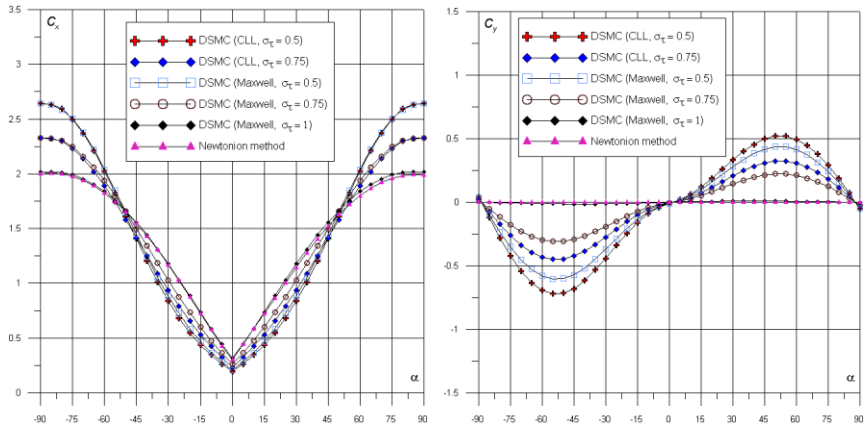

Figure 2.13 *Dependencies of $C_x(\alpha)$ and $C_y(\alpha)$ for aerospace vehicles.*

In figure 2.13 show the calculation results of the coefficients of drag force C_x, lift force C_y with value of angle of attack α from – 90 to + 90 deg for aerospace vehicle (Figure 2.12) are presented. The calculation has been carried out through the methods described in the previous section. The parameters of the problem are the following: ratio of heat capacities $\gamma = 1.4$; temperature factor $T_w/T_0 = 0.001$, $T_w/T_\infty = 0.1$; velocity ratio s = 15; accommodation coefficients $\sigma_\tau = 0.5, 0.75, 1$.

The Maxwell model and the Cercignani-Lampis-Lord model turned out to have principal differences, but in most cases they gave close values of aerodynamic forces and moments [48, 49].

In order to simulate the partial surface accommodation, the CLL model was implemented into this DSMC calculation. The CLL model is derived assuming momentum components. The two adjustable parameters appearing in the CLL model are the normal component of translational energy α_n and the tangential component of momentum σ_τ. However, in the implementation of the CLL model in the DSMC method, Bird has shown that it is equivalent to specify the normal

α_n and tangential α_τ components of translational energy, $\alpha_\tau=\sigma_\tau(2-\sigma_\tau)$ and $\sigma_\tau<\alpha_\tau$, assuming that σ_τ lies between 0 and 1.

For molecular velocity distributions, the Maxwell and CLL models gave similar ξ_x distributions, but distinct ξ_y distributions, at partial levels of gas-surface accommodation. Moreover, while the Maxwell scattering distributions experienced abrupt changes with increasing accommodation and position, the CLL distributions varied smoothly. For no significant additional cost, the CLL model gave more realistic scattering distributions.

The Investigation provided better understanding of the effects of gas-surface interaction models in DSMC calculations and ultimately a better understanding of the accommodation coefficients of materials and gases for orbital and aerobreaking conditions. The gas-surface interaction models have fundamental differences, they give similar predictions of aerodynamic forces on various aerospace vehicle design. The calculations with normal, tangential accommodation coefficients are provided more sensitivity of the aerothermodynamics quantities of aerospace technologies.